

Effect of Si/SiO₂ Interface on Silicon and Boron Diffusion in Thermally Grown SiO₂

Shigeto FUKATSU, Kohei M. ITOH*, Masashi UEMATSU¹, Hiroyuki KAGESHIMA¹,
Yasuo TAKAHASHI^{1,†} and Kenji SHIRAIISHI²

Department of Applied Physics and Physico-Informatics and CREST-JST, Keio University, Yokohama 223-8522, Japan

¹NTT Basic Research Laboratories, NTT Corporation, Atsugi 243-0198, Japan

²Institute of Physics, University of Tsukuba, Tsukuba 305-8571, Japan

(Received June 14, 2004; accepted August 20, 2004; published November 15, 2004)

Silicon self-diffusion and boron diffusion in SiO₂ were investigated as functions of the distance of diffusing silicon from the Si/SiO₂ interface at various temperatures in the range of 1150–1250°C using ^{nat}SiO₂/²⁸SiO₂ isotope heterostructures and ³⁰Si- and B-implanted ²⁸SiO₂ without and with a 30-nm-thick silicon nitride layer on the surface of each sample. The self-diffusivity of Si in SiO₂ did not depend on the oxygen concentration in the annealing ambient without the silicon nitride layer. The diffusion profiles of Si and B in the sample capped with the silicon nitride layer became broader as the distance from the Si/SiO₂ interface decreased. This dependence on the distance from the interface was caused by SiO molecules, which are generated at the interface and diffuse into SiO₂. The simulated results, taking into account the role of SiO molecules, showed good agreement with each experimental profile of ³⁰Si and B. [DOI: 10.1143/JJAP.43.7837]

KEYWORDS: silicon electronics, silicon dioxide, self-diffusion, gate insulator

1. Introduction

The diffusion phenomena in SiO₂ become important issues as the SiO₂ thickness decreases with the scaling down of Si metal oxide semiconductor (MOS) devices. For high-k gate dielectrics, diffusion in SiO₂ is important since a thin SiO₂ layer still exists between the Si and high-k materials. Si self-diffusion in SiO₂ is a fundamental phenomenon for the study of the oxide growth mechanism.^{1–3)} In addition, B diffusion in SiO₂ is an important issue because B penetrates through the thin gate oxide from the p⁺-polysilicon gate.^{4–6)}

Many studies on Si self-diffusion in SiO₂ have been conducted.^{7–14)} However, there is more than a one order of magnitude difference among the reported values of Si self-diffusivity ($D_{\text{Si}}^{\text{SD}}$).^{8,9,11–14)} The origin of the difference could be the existence of a silicon nitride (SiN) layer on the sample surface. It was considered that oxygen in an annealing ambient retards Si self-diffusion in SiO₂ without a SiN layer,¹³⁾ however, no experimental proof for that has been reported. We have investigated Si self-diffusion in SiO₂ as a function of oxygen concentration in an annealing ambient, using the ^{nat}SiO₂/²⁸SiO₂ isotope heterostructures without SiN (^{nat}Si refers to Si with natural isotopic abundance) and found that the oxygen molecules do not have an effect on Si self-diffusion. In §3, we discuss in detail the influence of oxygen in an annealing ambient on Si self-diffusion.

Moreover, we have investigated Si self-diffusion in ²⁸SiO₂ in which ³⁰Si were implanted as a function of the thickness of ²⁸SiO₂ using both a sample with a SiN layer and without it.⁷⁾ Surprisingly, we found that Si self-diffusion significantly depends on the thickness of ²⁸SiO₂ with the SiN layer but not on the thickness of the ²⁸SiO₂ without the SiN. Specifically, the diffusion profiles of Si became broader as the thickness of the ²⁸SiO₂ layers decreased, since Si self-diffusion is enhanced near the interface by SiO molecules generated at the interface.^{7,10)} From ref. 7, it is clear that this tendency is not caused by implantation damage and stress at the SiN/SiO₂ interface. A diffusion model that involves SiO

molecules has been constructed.¹⁰⁾ From the model, ³⁰Si diffusion profiles were simulated, and the results show good agreement with experimental profiles.¹⁰⁾ Moreover, the discrepancies among the reported values of Si self-diffusivity can be explained by taking into account the dependence of Si self-diffusion on the distance from the interface.⁷⁾ In §4, using the ^{nat}SiO₂/²⁸SiO₂ isotope heterostructures, which are different from the sample of ref. 7, we investigate Si self-diffusion as a function of the distance from the interface.

The question that we have to consider next is whether SiO molecules have an influence on B diffusion in SiO₂. B diffusion in SiO₂ has been investigated extensively with respect to the high concentration effect,¹⁵⁾ the effect of fluorine on B diffusion,¹⁶⁾ time dependence of B diffusion,¹⁷⁾ and mechanisms of B diffusion.^{18–20)} For thin gate oxides, it has been reported that B diffusion depends on the thickness of the oxide.²¹⁾ The dependence is probably caused by SiO molecules. In §5, we consider whether SiO molecules have an influence on B diffusion, using 200-, 300-, and 650-nm-thick ²⁸SiO₂ layers in which ³⁰Si and B were implanted.

2. Experimental

In this study, all samples were cut into into 5 × 5 mm² pieces and annealed in a resistance furnace under an appropriate condition, and the diffusion profiles of Si and B were measured by secondary ion mass spectroscopy (SIMS) using O₂⁺ ions as a primary ion beam with acceleration energy of 5 keV. The electron beam was irradiated on the sample during SIMS measurement to prevent the sample charging-up.

The samples used in the present work were prepared as follows. An isotopically enriched ²⁸Si epilayer of 800 nm thickness grown by chemical vapor deposition (CVD) was provided by Isonics Corp., Colorado, USA. The isotope composition measured with SIMS was ²⁸Si (99.924%), ²⁹Si (0.073%), and ³⁰Si (0.003%). The surface of the ²⁸Si epilayer was thermally oxidized in dry O₂ at 1100°C to form ²⁸SiO₂ of 200, 300, and 650 nm thicknesses. A simple ^{nat}SiO₂/²⁸SiO₂ isotope heterostructure was completed by deposition of ^{nat}SiO₂ of 50 nm thickness on the surface of ²⁸SiO₂ of 650 nm thickness by low-pressure chemical vapor

*E-mail address: kitoh@appi.keio.ac.jp

†Present address: Hokkaido University.

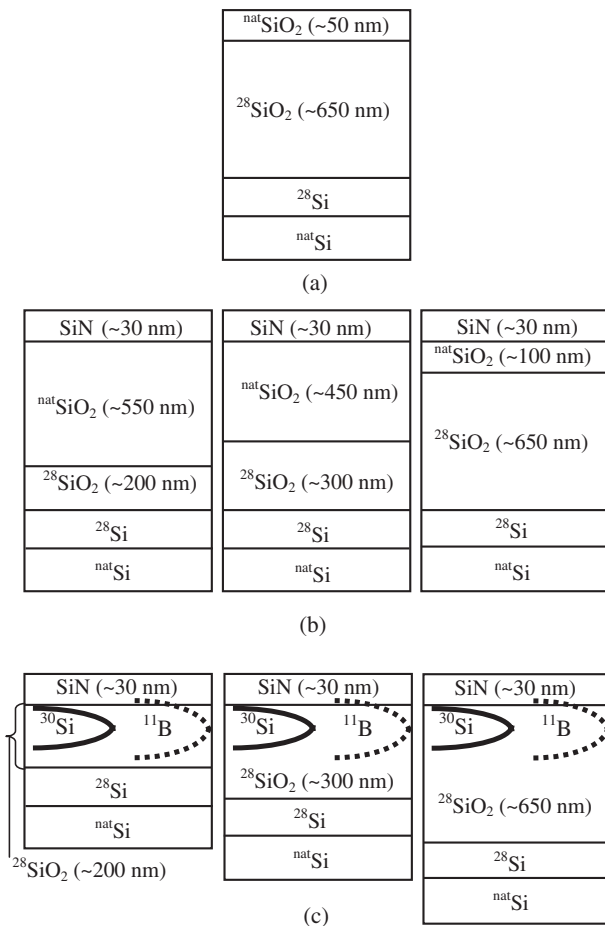


Fig. 1. Sample structures employed in this study: (a) isotope heterostructure without a SiN layer, (b) isotope heterostructures with a constant total oxide thickness, and (c) ^{30}Si - and ^{11}B -implanted $^{28}\text{SiO}_2$.

deposition (LPCVD) using tetraethoxysilane (TEOS) at 700°C , and the structure is shown in Fig. 1(a). The simple isotope heterostructure was cut and annealed at 1200 and 1250°C under flowing Ar with 1, 10, 50, 100% oxygen fractions in order to investigate the influence of the partial pressure of oxygen in an annealing ambient on Si self-diffusion in SiO_2 . The results of this experiment are discussed in §3.

$^{nat}\text{SiO}_2$ of 550, 450, and 100 nm thicknesses were deposited on the surfaces of $^{28}\text{SiO}_2$ of 200, 300, and 650 nm thicknesses, respectively, by LPCVD using TEOS at 700°C . The samples had the same total SiO_2 thickness (~750 nm). Finally, a 30-nm-thick silicon nitride layer was deposited on top of the samples by means of rf magnetron sputtering as shown in Fig. 1(b). The samples were annealed at 1200 and 1250°C under flowing Ar with a 1% oxygen fraction. In §4, we discuss the results of this experiment.

The thermally grown $^{28}\text{SiO}_2$ layers of 200, 300, and 650 nm thicknesses were implanted with ^{30}Si at 50 keV to a dose of $2 \times 10^{15} \text{ cm}^{-2}$ and capped with a ~30-nm-thick silicon nitride layer. Subsequently, the samples were implanted with ^{11}B at 25 keV to a dose of $5 \times 10^{13} \text{ cm}^{-2}$. The final structure is shown in Fig. 1(c). The samples were pre-annealed at 1000°C for 30 min to eliminate implantation damages, and annealed at various temperatures in the range of 1150 – 1250°C . In §5, we discuss the results of this experiment.

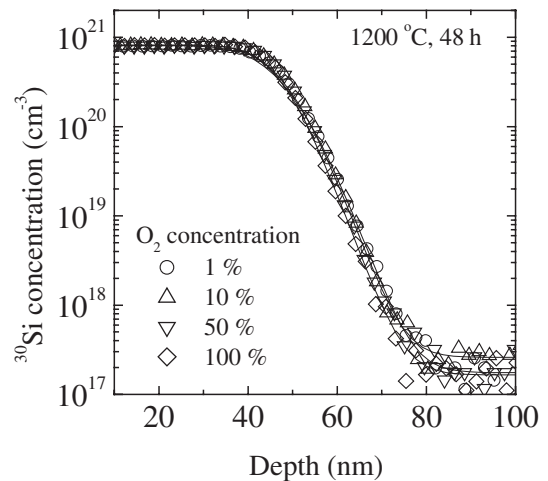


Fig. 2. SIMS results of isotope heterostructures without a SiN layer after annealing at 1200°C for 48 h with oxygen fractions of 1, 10, 50, and 100% in argon ambient. Solid curves are the fits of eq. (1).

3. Influence of Partial Pressure of Oxygen on Self-Diffusion of Si in SiO_2

At high temperature and low oxygen partial pressure, SiO_2 tends to decompose. In order to prevent decomposition of SiO_2 , Ar gas with 1% oxygen added has been used as the annealing ambient.^{7,8)} Mathiot *et al.* argued that annealing in an oxygen-containing ambient leads to lower self-diffusivity of Si.¹³⁾ In the present work, we investigated Si self-diffusion in SiO_2 as a function of the partial pressure of oxygen in the annealing ambient and found that Si self-diffusion does not depend on the partial pressure of oxygen.⁹⁾

The SIMS profiles of ^{30}Si are shown in Fig. 2. The results of various partial pressures of oxygen in the annealing ambient have almost the same profiles. This tendency was observed for the annealing at 1250°C . The solution of the diffusion equation for the isotope heterostructure is described by

$$C(x) = C_{^{28}\text{SiO}_2} + \frac{C_{^{nat}\text{SiO}_2} - C_{^{28}\text{SiO}_2}}{2} \times \left[\text{erf} \left(\frac{x+h}{2\sqrt{D_{\text{Si}}^{\text{SD}}(\text{th})t}} \right) - \text{erf} \left(\frac{x-h}{2\sqrt{D_{\text{Si}}^{\text{SD}}(\text{th})t}} \right) \right], \quad (1)$$

where $x = 0$ is the surface of the samples, $C_{^{28}\text{SiO}_2}$ and $C_{^{nat}\text{SiO}_2}$ are the concentrations of ^{30}Si in the $^{28}\text{SiO}_2$ layer and $^{nat}\text{SiO}_2$ layer, and h and t are the depth of the $^{nat}\text{SiO}_2/^{28}\text{SiO}_2$ interface and time, respectively. $D_{\text{Si}}^{\text{SD}}(\text{th})$, which is only a fitting parameter, is the Si self-diffusivity in SiO_2 under thermal equilibrium. Solid curves in Fig. 2 are the calculated ^{30}Si profiles. As shown in Fig. 3, the obtained values of $D_{\text{Si}}^{\text{SD}}(\text{th})$ after annealing in various partial pressures of oxygen were almost the same, and agreed with the values in ref. 8. The results indicate that the self-diffusivity of Si in SiO_2 does not depend on the partial pressure of oxygen in the annealing ambient. This is because diffusing oxygen in SiO_2 interacts minimally with silicon atoms forming the oxide network, and does not have an effect on Si self-diffusion in SiO_2 .⁹⁾

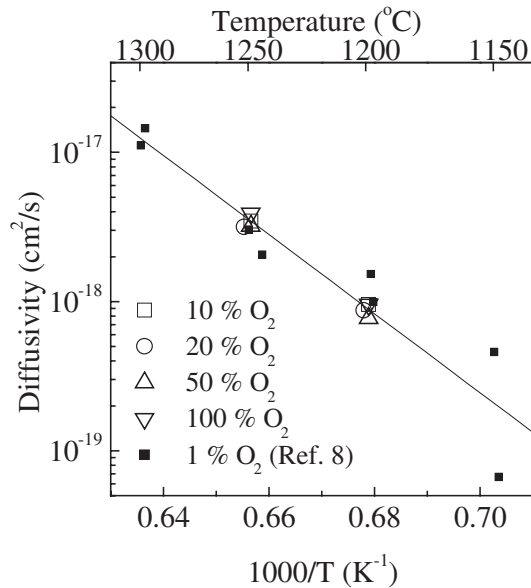


Fig. 3. Temperature dependence of Si self-diffusivity with oxygen fractions of 10, 20, 50, and 100% in argon ambient. The solid line corresponds to the value for 1% oxygen fraction in argon reported in ref. 8.

The results are consistent with the theoretical prediction that oxygen diffuses rapidly through predominantly the interstitial sites without interacting with Si atoms forming the SiO₂ network.²²⁾ Our experimental results, which contradict Mathiot's argument, indicated that oxygen in an annealing ambient does not have an influence on Si self-diffusion in SiO₂. The reason behind the contradiction is that Mathiot *et al.* did not take into account the effect of the Si/SiO₂ interface on Si self-diffusion. With a SiN cap, which acts as a diffusion barrier, on the SiO₂ surface, Si self-diffusion in the thin SiO₂ layer, in which the Si diffusers are near the Si/SiO₂ interface, is enhanced by SiO molecules which are generated at the interface.⁷⁾ On the other hand, without a SiN cap, Si self-diffusion in the thin SiO₂ is not enhanced by SiO molecules because few SiO molecules reach the ³⁰Si diffusers due to diffusing oxygen. Without the SiN cap, oxygen species incorporated into the SiO₂ from the oxygen containing annealing ambient diffuse across the SiO₂. When oxygen molecules arrive at the Si/SiO₂ interface region, they recombine with the SiO molecules generated from the interface to form the additional SiO₂.¹⁷⁾ Therefore, the SiO molecules do not reach the ³⁰Si diffusers, and there is no enhancement of Si self-diffusion when SiO₂ is not capped with the SiN layer.

Our experiment clearly shows that the oxygen diffusion does not have a direct influence on Si self-diffusion in SiO₂. Si self-diffusion in the thin SiO₂ layer is slower without the SiN cap than that with it. Containing oxygen in the annealing ambient does not retard Si self-diffusion but prevents the enhancement of Si self-diffusion.

4. Effect of the Si/SiO₂ Interface on Si Self-Diffusion in SiO₂

We have experimentally shown the dependence of Si self-diffusion in SiO₂ capped with SiN on the distance from the Si/SiO₂ interface using the ³⁰Si-implanted ²⁸SiO₂ layer of

200, 300, and 650 nm thicknesses.⁷⁾ The dependence is as follows. With the SiN layer on the surface, the Si self-diffusivity increases as the ²⁸SiO₂ thickness decreases. On the other hand, without the SiN layer, the Si self-diffusivity does not depend on the thickness, and the values of the diffusivity agree with the thermal Si self-diffusivity ($D_{\text{Si}}^{\text{SD(th)}}$).⁸⁾ Specifically, with the SiN layer, the values obtained using the samples with the 650-nm-thick ²⁸SiO₂ layer also showed good agreement with the $D_{\text{Si}}^{\text{SD(th)}}$.

In the present work, using the ^{nat}SiO₂/²⁸SiO₂ isotope heterostructures, as shown in Fig. 1(b), the effect of the Si/SiO₂ interface was investigated. The objective of this experiment is to experimentally confirm that Si self-diffusion in SiO₂ does not depend on the oxide thickness but on the distance between ³⁰Si diffusers and the Si/SiO₂ interface. In the previous study,⁷⁾ the oxide thickness was changed in order to vary the distance, while in the isotope heterostructures used in the present study, the total oxide thicknesses were the same (~750 nm), as shown in Fig. 1(b).

Figures 4(a) and 4(b) show the SIMS profiles of ³⁰Si in the isotope heterostructures after diffusion annealing. In these isotope heterostructures, the total oxide thickness of each sample was almost the same, while the thickness of the ²⁸SiO₂ layer of each sample was varied: the distance between the ^{nat}SiO₂/²⁸SiO₂ interface, at which Si self-diffusion was observed, and the ²⁸Si/²⁸SiO₂ interface was different. In Fig. 4(b), the profiles were shifted along the *x*-axis in order that each ^{nat}SiO₂/²⁸SiO₂ interface would agree at *x* = 0. Figure 4(b) indicates that the diffusion length of the sample with the 200-nm-thick ²⁸SiO₂ layer, the thinnest ²⁸SiO₂ layer in this work, was longer than that of other samples. This tendency was observed at other temperatures, and is consistent with the finding that Si self-diffusivity increases as the distance between the Si/SiO₂ interface and the ^{nat}SiO₂/²⁸SiO₂ interface decreases.^{7,10)} As mentioned above, these samples have the same total oxide thickness; therefore, Si self-diffusivity in SiO₂ does not depend on the oxide thickness but on the distance between the diffusers and the Si/SiO₂ interface, as mentioned in refs. 7 and 10.

The mechanism of the dependence of Si self-diffusion is interpreted as follows.¹⁰⁾ SiO molecules are generated at the interface via $\text{Si} + \text{SiO}_2 \rightarrow 2\text{SiO}$ ^{23,24)} and diffuse into oxide, which has been predicted by various studies.^{2,23–26)} SiO diffusion is not so fast that the concentration of SiO molecules becomes uniform in the 200-nm-thick oxide but is much faster than Si self-diffusion.^{10,23,27)} Therefore, the diffusion of Si atoms via SiO is faster than the thermal Si self-diffusion where Si atoms do not diffuse via SiO, and the higher the SiO concentration, the faster the diffusion of Si atoms. The concentration of SiO increases as the distance from the interface at which SiO molecules are generated decreases. As a result, Si self-diffusion is enhanced near the interface, where the concentration of SiO molecules is high.

An analysis of Si self-diffusion was conducted in a manner similar to that in ref. 10. The diffusion equations for ³⁰Si, ³⁰SiO, and ²⁸SiO were solved numerically.¹⁰⁾ In the simulation, SiO molecules were taken into account as:



Equation 2 indicates that Si atoms substituted into Si sites of

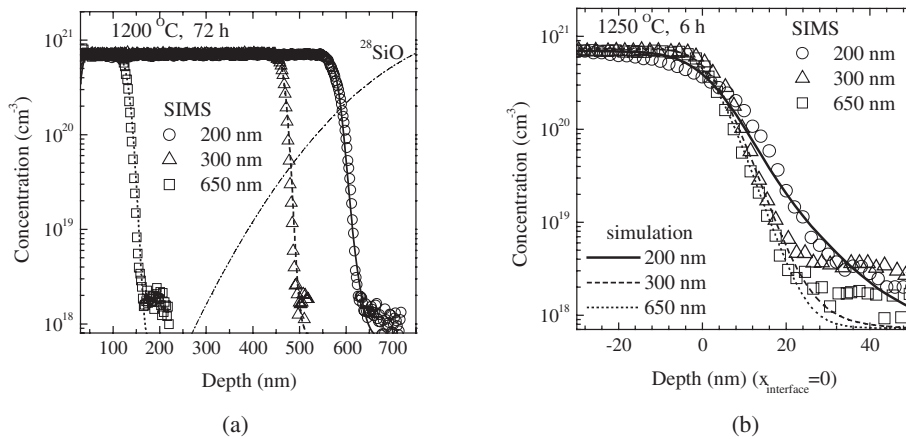


Fig. 4. SIMS results for the isotope heterostructures with a constant total oxide thickness: (a) raw profiles, (b) shifted along x -axis so that each interface between $^{nat}\text{SiO}_2$ and $^{28}\text{SiO}_2$ agrees at $x = 0$. Open circles, open triangles, and open squares represent the SIMS depth profiles of the samples with 200-, 300-, and 650-nm-thick $^{28}\text{SiO}_2$ layers. The chain line is the profile of ^{28}SiO molecules obtained by the simulation. The rest of the lines are simulated ^{30}Si profiles for each structure.

SiO_2 [denoted as (sub)] diffuse via the kick-out mechanism, reacting with diffusing SiO molecules in interstitial sites [denoted as (int)]. In addition, Si atoms diffuse via a mechanism which does not involve SiO . The Si self-diffusivity is therefore described by

$$D_{\text{Si}}^{\text{SD}} = D_{\text{Si (th)}}^{\text{SD}} + D_{\text{SiO}}^{\text{SD}} C_{\text{SiO}}^{\circ} / C_{\text{SiO}_2}^{\circ}, \quad (3)$$

where C_{SiO}° is the maximum concentration of SiO in SiO_2 and is described as $C_{\text{SiO}}^{\circ} = 3.6 \times 10^{24} \exp(-1.07 \text{ eV}/kT)$.¹⁰ $D_{\text{SiO}}^{\text{SD}} = D_{\text{SiO}} C_{\text{SiO}}^{\circ} / N_o$ is the self-diffusivity of silicon via SiO molecules, where N_o denotes the number of SiO_2 molecules in a unit volume of SiO_2 . $D_{\text{Si (th)}}^{\text{SD}}$ is the Si self-diffusivity via the mechanism which does not involve SiO molecules, and $D_{\text{Si (th)}}^{\text{SD}} = 0.8 \exp(-5.2 \text{ eV}/kT) \text{ cm}^2/\text{s}$.^{8,9} was used in the present study. The boundary condition for $^{28}\text{SiO}(\text{int})$ at the $^{28}\text{Si}/^{28}\text{SiO}_2$ interface is given by $C_{^{28}\text{SiO}} = C_{\text{SiO}}^{\circ}$ to describe the generation of SiO at the interface. The amount of $^{30}\text{SiO}(\text{int})$ arriving at the $^{28}\text{Si}/^{28}\text{SiO}_2$ interface is so small that the mixing of ^{28}Si with ^{30}Si at the interface can be neglected. The boundary condition at the nitride-capped surface is represented by a zero-flux condition because the caps act as barriers. It is reasonable to assume that reaction (2) is so fast that the local equilibrium of the reaction is established, and hence, the rate constants are set to be sufficiently large. The only parameter obtained from the simulation to fit the experimental profiles of ^{30}Si is D_{SiO} . In addition, in our calculation, the broadening of SIMS profiles caused by surface roughness and mixing by SIMS sputtering was taken into account using the method developed by Hoffman.²⁸⁾

Simulated results show good agreement with the experimental profiles, as shown in Figs. 4(a) and 4(b). Therefore, the dependence of Si self-diffusion in the isotope heterostructures on the distance can be explained by taking into account SiO molecules. The diffusivity of SiO (D_{SiO}) obtained in the present work agrees with $D_{\text{SiO}} = 3.4 \times 10^2 \exp(-5.2 \text{ eV}/kT) \text{ cm}^2/\text{s}$ of ref. 10, as shown in Fig. 5. Si self-diffusion in the isotope heterostructures and in the ^{30}Si -implanted $^{28}\text{SiO}_2$ layers can be simulated by using the same values of D_{SiO} . The samples used in the present work had almost the same total oxide thickness; the only difference

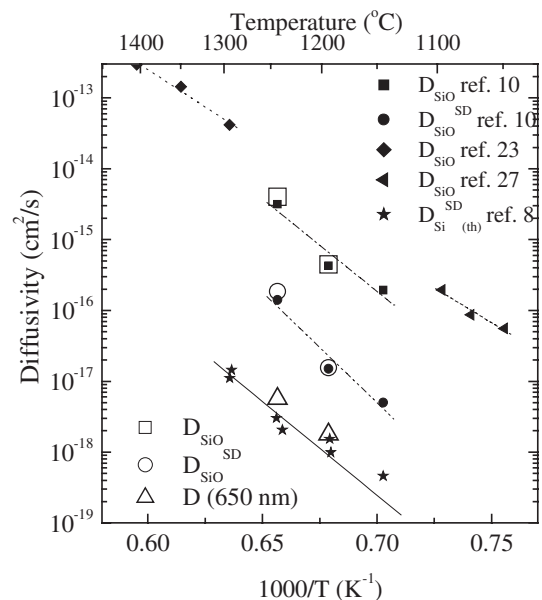


Fig. 5. Diffusivity in SiO_2 as a function of temperature. Open squares, open circles, and open triangles, which indicate the values obtained in the present work, are the SiO diffusivity (D_{SiO}), Si self-diffusivity via SiO ($D_{\text{SiO}}^{\text{SD}}$), and the thermal Si self-diffusivity ($D_{\text{Si (th)}}^{\text{SD}}$). Filled circles represent the results of $D_{\text{SiO}}^{\text{SD}}$ obtained by the simulation in ref. 10. The results of the determination of D_{SiO} using ^{30}Si as markers (filled squares) (ref. 10), in CVD SiO_2 using thermally migrated impurities as markers (filled triangles) (ref. 27), and using defect evolutions as markers (filled diamonds) (ref. 23) are also shown.

among the samples was the distance from the $^{28}\text{Si}/^{28}\text{SiO}_2$ interface. Therefore, the distance has a significant effect on Si self-diffusion, as mentioned.^{7,10} Experimentally, we have confirmed that Si self-diffusion in SiO_2 does not depend on the total oxide thickness but on the distance between ^{30}Si diffusers and the Si/SiO_2 interface.

The calculated profiles of ^{28}SiO are also shown in Fig. 4(a). After the annealing at 1200°C for 72 h, the concentration of SiO molecules arriving from the Si/SiO_2 interface was $\sim 10^{20} \text{ cm}^{-3}$ at the $^{nat}\text{SiO}_2/^{28}\text{SiO}_2$ interface of the sample with the 200-nm-thick $^{28}\text{SiO}_2$ layer. As a result, Si self-diffusion was enhanced in the sample by the high

concentration of SiO molecules. For the samples with the 650-nm-thick $^{28}\text{SiO}_2$ layer, few SiO molecules arrived at the $^{\text{nat}}\text{SiO}_2/^{28}\text{SiO}_2$ interface. Since enhancement of Si self-diffusion by SiO molecules is negligible, the analysis assuming a constant Si self-diffusivity is valid for the samples. The diffusivity obtained for the samples agrees with the $D_{\text{Si}}^{\text{SD}} = 0.8 \exp(-5.2 \text{ eV}/kT) \text{ cm}^2/\text{s}$ of Takahashi *et al.*⁸⁾ as shown in Fig. 5. The results were obtained with the SiN layer, which acts as barrier to oxygen diffusion, and the diffusivity agrees with the value of Si self-diffusivity reported in refs. 8 and 9. Therefore, the residual oxygen in an ambient does not have an influence on Si self-diffusion in SiO_2 , as mentioned above.

As we argued in ref. 7, it is confirmed here that there is no effect of the stress between the SiN layer and SiO_2 on Si self-diffusion since the same value of $D_{\text{Si}}^{\text{SD}}$ can be used for the simulation of all the samples with various distances between the SiN/ SiO_2 interface and the $^{\text{nat}}\text{SiO}_2/^{28}\text{SiO}_2$ interface.

5. Effect of the Si/ SiO_2 Interface on Boron Diffusion in SiO_2

In this section, we have investigated the effect of the Si/ SiO_2 interface on B diffusion using the B-implanted samples shown in Fig. 1(c). Originally, we have coimplanted ^{30}Si with B in order to investigate the effect of B diffusion on Si self-diffusion in SiO_2 . However, we have found recently that Si self-diffusion is affected only by B of concentration larger than 10^{20} cm^{-3} .³¹⁾ Therefore, we employed ^{30}Si with less than 10^{19} cm^{-3} as an additional marker to ensure the accuracy of our experiments. Figure 6 shows the depth profiles of ^{11}B before and after annealing at 1200°C for 24 h. The profiles after the pre-annealing agree with the as-implanted profiles within the experimental error of our SIMS measurements.

The profiles of ^{11}B became broader with decreasing $^{28}\text{SiO}_2$ layer thickness, i.e., B diffusivity increased with decreasing distance from the Si/ SiO_2 interface, as shown in Fig. 6. This tendency was observed for other temperatures

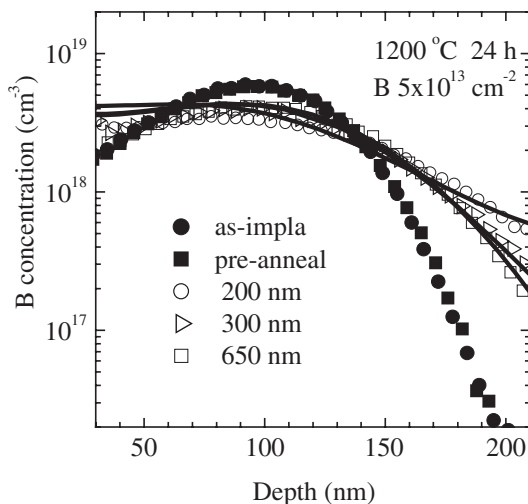
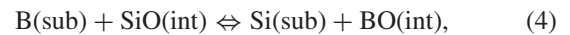


Fig. 6. Simulated (solid line) and experimental ^{11}B profiles after annealing at 1200°C for 24 h. As initial profiles, the profiles of as-implanted and pre-annealed samples are also shown. The smaller the distance between implanted B and the Si/ SiO_2 interface is, the broader the B profile becomes.

probed in this study. The dependence of B diffusion in SiO_2 on the distance from the Si/ SiO_2 interface is similar to that of Si self-diffusion in SiO_2 .⁷⁾ As mentioned above, Si self-diffusion is enhanced by SiO molecules generated at the interface and diffusing into the oxide. The shorter the distance between implanted B and the interface, at which the SiO concentration is high, becomes, the broader the B diffusion profiles become. In order to confirm whether the origin of B diffusion enhancement is the effect of SiO molecules, we have constructed the model of B diffusion taking into account SiO molecules, and compared the results of the simulation based on the model with SIMS profiles.

The B diffusion model was proposed as a natural extension of a previously proposed model of Si self-diffusion.¹⁰⁾ The results in Fig. 6 indicate that B diffuses via a mechanism that involves SiO in addition to one that does not involve SiO. An evidence for the existence of two mechanisms is that very few SiO molecules arrived from the interface in the 650-nm-thick samples. B diffusion via SiO can be described as



in a similar manner to B diffusion in Si via the kick-out mechanism, where $\text{BO}(\text{int})$ may be a complex of Si-B-O.¹⁸⁾ The SiO concentration is high near the interface during annealing, therefore, the large contribution of relatively rapid B diffusion via SiO leads to higher total B diffusivity.

From the model, the diffusion equations were constructed and numerically solved by the partial differential equation solver ZOMBIE.²⁹⁾ Taking into account the two mechanisms, the total effective B diffusivity is described by

$$D_{\text{B}}^{\text{eff}} = D_{\text{B}(\text{th})}^{\text{eff}} + D_{\text{i}}^{\text{eff}} C_{\text{SiO}}/C_{\text{SiO}}^{\circ}, \quad (5)$$

where $D_{\text{B}(\text{th})}^{\text{eff}}$ and $D_{\text{i}}^{\text{eff}}$ are the effective diffusivity of thermal B diffusion and the effective diffusivity of B diffusion via the mechanism that involves SiO molecules. The experimentally obtained effective diffusivity of thermal B diffusion, $D_{\text{B}(\text{th})}^{\text{eff}} = 3.12 \times 10^{-3} \exp(-3.93 \text{ eV}/kT) \text{ cm}^2/\text{s}$ ³⁰⁾ was used. $D_{\text{SiO}}^{\text{SD}} = 4 \times 10^4 \exp(-6.2 \text{ eV}/kT) \text{ cm}^2/\text{s}$ ¹⁰⁾ was applied in this simulation. As a result, the parameter to be obtained by fitting is $D_{\text{i}}^{\text{eff}}$.

Figure 6 shows that the simulation results for the all $^{28}\text{SiO}_2$ thicknesses agree with the experimental results. Therefore, the dependence of B diffusion on the distance from the Si/ SiO_2 interface can be explained by taking into account SiO molecules. However, the experimentally obtained B profiles near the SiN/ $^{28}\text{SiO}_2$ interface in SiO_2 do not agree perfectly with the simulated profiles. This may be due to boron segregation at the SiN/ $^{28}\text{SiO}_2$ interface as reported previously.³²⁾

In the present work, ^{30}Si diffusion profiles in the B-implanted $^{28}\text{SiO}_2$ layers agreed fairly with that of the $^{28}\text{SiO}_2$ layers without B implantation,⁷⁾ as shown in Fig. 7. Implanted B and B diffusion do not have an influence on Si self-diffusion at the concentration employed in the present work since the B concentration was lower than 10^{20} cm^{-3} .³¹⁾

6. Conclusion

First, we have shown that Si self-diffusion in SiO_2 without SiN does not depend on the partial pressure of oxygen in the annealing ambient. Next, the effect of the Si/ SiO_2 interface

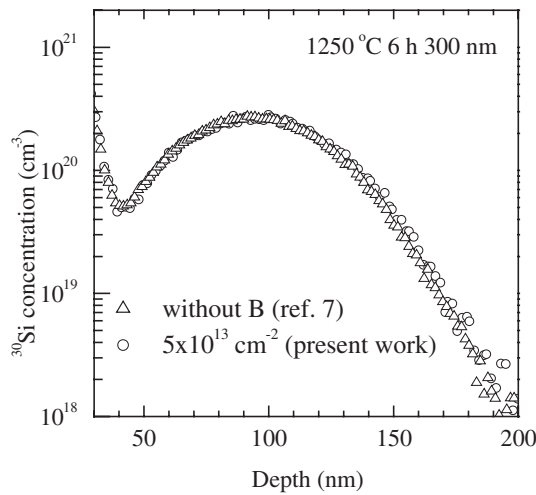


Fig. 7. Diffusion profiles of ^{30}Si in the $^{28}\text{SiO}_2$ layers with B implantation (open circles) and without B implantation (open triangles).

on Si self-diffusion in SiO_2 was investigated using isotope heterostructures with a constant total oxide thickness. With the SiN layer, Si self-diffusion was enhanced near the interface in a manner similar to that in ^{30}Si -implanted samples. For both samples, Si self-diffusion can be simulated using the same value of the diffusivity of SiO. Therefore, we have confirmed that the enhancement of Si self-diffusion depends on the distance between the ^{30}Si diffusers and the Si/SiO₂ interface, as argued in refs. 7 and 10. Moreover, we have shown that B diffusion in SiO₂ is also enhanced near the interface. By taking into account SiO molecules, a simulation was performed for Si and B diffusion, and the results showed good agreement with the experimental profiles. Therefore, the enhancement mechanism is that SiO molecules generated at the interface and diffusing into SiO₂ enhance B diffusion as well as Si self-diffusion. SiO diffusion is faster than Si self-diffusion in SiO₂, but is not so fast that the SiO concentration becomes constant all over the SiO₂ layer. Since the concentration of SiO molecules is higher near the interface, the enhancements of Si self-diffusion and B diffusion in SiO₂ are larger near the interface.

Acknowledgments

We thank U. Gösele and K. Yamada for fruitful discussions, H. Inokawa for B implantations, K. Nishiguchi for CVD, and A. Takano for SIMS measurements. The work was supported in part by a Grant-in-Aid for Scientific Research Nos. 14076215 and 14550020, and by “High-k Network” in cooperation with academic, industry, and government institutions.

- 1) H. Kageshima and K. Shiraishi: Phys. Rev. Lett. **81** (1998) 5936.
- 2) H. Kageshima, K. Shiraishi and M. Uematsu: Jpn. J. Appl. Phys. **38** (1999) L971.
- 3) M. Uematsu, H. Kageshima and K. Shiraishi: Jpn. J. Appl. Phys. **39** (2000) L699.
- 4) K. Suzuki, A. Satoh, T. Aoyama, I. Namura, F. Inoue, Y. Kataoka, Y. Tada and T. Sugii: J. Electrochem. Soc. **142** (1995) 2786.
- 5) T. Aoyama, K. Suzuki, H. Tashiro, Y. Tada and H. Arimoto: Tech. Dig. Int. Electron Devices Meet. IEDM-97 (1997) p. 627.
- 6) M. Cao, P. Vande Voorde, M. Cox and W. Greene: IEEE Electron Device Lett. **19** (1998) 291.
- 7) S. Fukatsu, T. Takahashi, K. M. Itoh, M. Uematsu, A. Fujiwara, H. Kageshima, Y. Takahashi, K. Shiraishi and U. Gösele: Appl. Phys. Lett. **83** (2003) 3897.
- 8) T. Takahashi, S. Fukatsu, K. M. Itoh, M. Uematsu, A. Fujiwara, H. Kageshima, Y. Takahashi and K. Shiraishi: J. Appl. Phys. **93** (2003) 3674.
- 9) S. Fukatsu, T. Takahashi, K. M. Itoh, M. Uematsu, A. Fujiwara, H. Kageshima, Y. Takahashi and K. Shiraishi: Jpn. J. Appl. Phys. **42** (2003) L1492.
- 10) M. Uematsu, H. Kageshima, Y. Takahashi, S. Fukatsu, K. M. Itoh, K. Shiraishi and U. Gösele: Appl. Phys. Lett. **84** (2004) 876.
- 11) G. Brebec, R. Seguin, C. Sella, J. Bevenot and J. C. Martin: Acta Metall. **28** (1980) 327.
- 12) O. Jaoul, F. Béjina, F. Élie and F. Abel: Phys. Rev. Lett. **74** (1995) 2038.
- 13) D. Mathiot, J. P. Schunck, M. Perego, M. Fanciulli, P. Normand, C. Tsamis and D. Tsoukalas: J. Appl. Phys. **94** (2003) 2136.
- 14) D. Tsoukalas, C. Tsamis and P. Normand: J. Appl. Phys. **89** (2001) 7809.
- 15) T. Aoyama, H. Arimoto and K. Horiuchi: Jpn. J. Appl. Phys. **40** (2001) 2685.
- 16) T. Aoyama, K. Suzuki, H. Tashiro, Y. Toda, T. Yamazaki, K. Takasaki and T. Ito: J. Appl. Phys. **77** (1995) 417.
- 17) K. A. Ellis and R. A. Buhrman: Appl. Phys. Lett. **74** (1999) 967.
- 18) M. Otani, K. Shiraishi and A. Oshiyama: Phys. Rev. Lett. **90** (2003) 075901.
- 19) M. Otani, K. Shiraishi and A. Oshiyama: Phys. Rev. B **68** (2003) 184112.
- 20) R. B. Fair: J. Electrochem. Soc. **144** (1997) 708.
- 21) R. B. Fair: IEEE Electron. Device Lett. **17** (1996) 242.
- 22) W. Orellana, A. J. R. da Silva and A. Fazzio: Phys. Rev. Lett. **87** (2001) 155901.
- 23) G. K. Celler and L. E. Trimble: Appl. Phys. Lett. **54** (1989) 1427.
- 24) T. Y. Tan and U. Gösele: Appl. Phys. Lett. **40** (1982) 616.
- 25) A. M. Stoneham, C. R. M. Grovenor and A. Cerezo: Philos. Mag. B **55** (1987) 201.
- 26) Y. Takakuwa, M. Nihei and N. Miyamoto: Appl. Surf. Sci. **117/118** (1997) 141.
- 27) D. Tsoukalas, C. Tsamis and J. Stoemenos: Appl. Phys. Lett. **63** (1993) 3167.
- 28) S. Hofmann: Surf. & Interfaces Anal. **21** (1994) 673.
- 29) W. Jüngling, P. Pichler, S. Selberherr, E. Guerrero and H. W. Pötzel: IEEE Trans. Electron Devices **32** (1985) 156.
- 30) T. Aoyama, H. Tashiro and K. Suzuki: J. Electrochem. Soc. **146** (1999) 1879.
- 31) M. Uematsu, H. Kageshima, Y. Takahashi, S. Fukatsu, K. M. Itoh and K. Shiraishi: Appl. Phys. Lett. **85** (2004) 221.
- 32) G. Charitat and A. Martinez: J. Appl. Phys. **55** (1984) 2869.